CrossMark

AglH, a thermophilic UDP-*N*-acetylglucosamine-1-phosphate: dolichyl phosphate GlcNAc-1-phosphotransferase initiating protein *N*-glycosylation pathway in *Sulfolobus acidocaldarius*, is capable of complementing the eukaryal AlgH

Benjamin H. Meyer[1,3] · Hosam Shams-Eldin[2] · Sonja-Verena Albers[1]

Abstract AglH, a predicted UDP-GlcNAc-1-phosphate: dolichyl phosphate GlcNAc-1-phosphotransferase, is initiating the protein *N*-glycosylation pathway in the thermoacidophilic crenarchaeon *Sulfolobus acidocaldarius*. AglH successfully replaced the endogenous GlcNAc-1-phosphotransferase activity of Alg7 in a conditional lethal *Saccharomyces cerevisiae* strain, in which the first step of the eukaryal protein *N*-glycosylation process was repressed. This study is one of the few examples of cross-domain complementation demonstrating a conserved polyprenyl phosphate transferase reaction within the eukaryal and archaeal domain like it was demonstrated for *Methanococcus voltae* (Shams-Eldin et al. 2008). The topology prediction and the alignment of the AglH membrane protein with GlcNAc-1-phosphotransferases from the three domains of life show significant conservation of amino acids within the different proposed cytoplasmic loops. Alanine mutations of selected conserved amino acids in the putative cytoplasmic loops II (D_{100}), IV (F_{220}) and V (F_{264}) demonstrated the importance of these amino acids for cross-domain AglH activity in in vitro complementation assays in *S. cerevisiae*. Furthermore, antibiotic treatment interfering directly with the activity of dolichyl phosphate GlcNAc-1-phosphotransferases confirmed the essentiality of *N*-glycosylation for cell survival.

Keywords *N*-Glycosylation · Crenarchaea · *Sulfolobus* · Glycosylation · Dolichol phosphate · Alg7 · AglH

Communicated by A. Driessen.

✉ Sonja-Verena Albers
  sonja.albers@biologie.uni-freiburg.de

1 Molecular Biology of Archaea, Institute of Biology, University of Freiburg, Schaenzlestrasse 1, 79211 Freiburg, Germany

2 Institute of Virology, Hans-Meerwein-Str. 2, 35043 Marburg, Germany

3 Present Address: Division of Molecular Microbiology, School of Life Sciences, University of Dundee, Dundee DD1 5EH, UK

Introduction

All living cells exhibit an outer surface covered with an array of glycans. These glycans are either loosely attached or covalently linked to surface proteins or lipids. Protein glycosylation is one of the most common posttranslational protein modifications found in all three domains of life (Larkin and Imperiali 2011). In particular, protein *N*-glycosylation is widely distributed in Eukarya and Archaea whereas it is rarely found in Bacteria. In these systems, the biosynthesis of *N*-linked oligosaccharides is initiated by the transfer of a sugar(-1-phosphate) residue from a nucleotide-activated sugar onto the lipid carrier dolichyl phosphate (DolP) or undecaprenyl phosphate (UndP), respectively. The fully assembled lipid-linked glycan is then transferred to a specific Asn (*N*) residue within a target protein.

Eukaryotic protein *N*-glycosylation is initiated by the GlcNAc-1-phosphate transferase Alg7/Dpagt1 (Lehrman 1991; Mclachlan and Krag 1992), which converts UDP-GlcNAc and DolP into UMP and DolPP-GlcNAc. This step is essential in Eukarya and defined mutations in the human Dpagt1 cause severe clinical phenotypes, leading to lethal diseases (Jaeken and Matthijs 2007; Wurde et al. 2012). DolPP-GlcNAc acts as a primer for the elongation

of the N-glycans by specific glycosyltransferases (GTases), sequentially transferring individual sugars from corresponding nucleotide- or lipid phosphate-activated precursors (Burda and Aebi 1999).

The bacterial protein N-glycosylation pathway from *Campylobacter jejuni* starts with the transfer of diacetamido bacillosamine-1-P from UDP-2,4-diacetamido bacillosamine onto the lipid carrier UndP by the phosphotransferase PglC (Glover et al. 2006). Similar to the initiation of protein N-glycosylation, the biosynthesis of several other bacterial glycoconjugates starts at the cytoplasmic site of the cell membrane with the formation of an UndPP-linked monosaccharide. Examples include the biosynthesis of O-antigen polymers (Meier-Dieter et al. 1992; Samuel and Reeves 2003; Schmidt et al. 1976), the capsular antigens (Masson and Holbein 1985; Troy et al. 1975; Whitfield 2006), lipopolysaccharide (Alexander and Valvano 1994; Schmidt et al. 1976), teichoic acids (Brown et al. 2008; Ginsberg et al. 2006; Mancuso and Chiu 1982) and the peptidoglycan (Bouhss et al. 2008; Bugg and Brandish 1994; Typas et al. 2012). The initiation step is mediated by different classes of membrane-bound UDP-hex(NAc)-1-phosphate:polyprenyl phosphate sugar-1-phosphotransferase enzymes, which use UndP as an acceptor but differ in their specificity for the nucleotide sugar donor. The bacterial enzyme WecA (formerly known as Rfe) catalyses the first step of biosynthesis of many LPS O-antigens and capsular K-antigens by the transfer of GlcNAc-1-P residue from UDP-GlcNAc onto UndP (Amor and Whitfield 1997).

In Archaea, N-glycosylation pathways for three different euryachaea and one crenarchaeon have been described [for review see (Jarrell et al. 2014)]. In contrast to Eukarya and Bacteria, most of the euryarchaeal N-glycans characterised to date, i.e. *Hfx. volcanii*, *Haloarcula marismortui*, *Methanococcus voltae*, and *Pyrococcus furiosus*, are assembled on DolP lipid carrier (Calo et al. 2011; Chang et al. 2015; Guan et al. 2010; Larkin et al. 2013), with two exceptions. *Methanothermus fervidus* assemble their N-glycans on DolPP (Hartmann and König 1989) and *Hbt. salinarum*, which synthesizes two distinct N-glycans, assembles one on DolP and the second on DolPP (Paul and Wieland 1987). A recent comparison of archaeal lipid-linked oligosaccharides revealed a difference between eury- and crenarchaeota. Indeed, selected species of the euryarchaeota

possessed DolP-linked glycans, whereas the crenarchaeota *Pyrobaculum calidifontis* and *Sulfolobus solfataricus* assemble their N-glycans on DolPP (Taguchi et al. 2016). Different steps of the N-glycosylation pathway of the closely related crenarchaeon *Sulfolobus acidocaldarius* have been studied in detail (Meyer and Albers 2013). Here, a tribranched hexasaccharide, composed of two GlcNAc, two terminal Man, one sulfoquinovose and one terminal Glc are found as the N-glycan linked to the S-layer protein (Peyfoon et al. 2010). Interestingly, the basal structure of this archaeal N-glycan ($GlcNAc_2Man$) resembles this of the eukaryal one and the biosynthesis might rely on homologs to the eukaryal ones.

Unlike in euryarchaeota, the initiation step of the protein N-glycosylation process in thermophilic crenarchaeota has not yet been elucidated. In the present study, we identified a candidate enzyme for the initiation step of the protein N-glycosylation pathway in *S. acidocaldarius* by homology searches. The identified AglH (Saci0093) is able to restore N-glycosylation in a conditional lethal *Saccharomyces cerevisiae alg*7 mutant. Various attempts to delete *aglH* in *S. acidocaldarius* were unsuccessful, and the use of tunicamycin, a specific inhibitor of UDP-HexNAc-1-phosphate:polyprenol phosphate HexNAc-1-phosphotransferases, as well as the treatment with bacitracin interfering with the regeneration of DolP, revealed the essentiality of AglH in *S. acidocaldarius*.

Materials and methods

Strains and growth conditions

Sulfolobus acidocaldarius background strain MW001 (∆*pyrE*) (Wagner et al. 2012) and the genetically-modified strains *S. acidocaldarius* BM-A120-124 (see Table 1) were grown under shaking conditions in Brock medium at 79 °C, pH 3, and supplemented with 0.1% w/v NZ amine and 0.1% w/v dextrin as carbon and energy source (Brock et al. 1972). For the uracil auxotrophic strains, the growth medium was supplemented with 10 mg ml^{-1} uracil. Gelrite (0.6%) plates were supplemented with the same nutrients, with the addition of 10 mM $MgCl_2$ and 3 mM $CaCl_2$. For second selection plates, 10 mg ml^{-1}

Table 1 Strains used in this study

Strain	Genotype	References
MW001	*S. acidocaldarius* DSM 639 ∆*pyrE*	Wagner et al. (2012)
BM-A120-124	MW001 strain with the integrated plasmid pSVA1229	This study
YPH499-HIS-GAL-ALG7	Mat *a*; ura3-52; lys2-801[amber]; ade2 ± 101[ochre] trpl-D63; his3-D200; leu2-D1, GAL-ALG7	Mazhari-Tabrizi et al. (1999)

uracil and 100 mg ml^{-1} 5-fluoroorotic acid (5-FOA) were added. Growth of the cultures was monitored by measuring the optical density at 600 nm. The *S. cerevisiae* strains YPH499-HIS-GAL-ALG7 (Mazhari-Tabrizi et al. 1999) used as a control and recipient strain, as well as the complementation strains were grown either in SD medium (2% dextrose, 0.17% Bacto yeast nitrogen base) (repression medium) or in SGR-His medium (4% galactose, 2% raffinose, 0.17% Bacto yeast nitrogen base, 0.5% ammonium sulphate) (non-selective medium). The 1.5% agar plates containing either SGR or SD medium were used for the complementation assay.

Growth studies with bacitracin and tunicamycin

Pre-cultures grown to an OD$_{600}$ of 0.4–0.5 were used to inoculate 5 ml of fresh Brock medium (0.1% w/v NZ amine and 0.1% w/v dextrin) to a start OD of 0.01. Directly with inoculation or after reaching exponential growth phase, different concentrations of the antibiotics bacitracin (0.6, 1.2, and 2.4 mM) and tunicamycin (2, 6, 16, and 32 µg/ml) were added. Growth was monitored by measuring the OD$_{600}$ over a time period of 80 h.

Construction of a Δ*aglH* deletion

A markerless deletion mutant would represent an important tool to analyse whether the predicted UDP-GlcNAc-1-phosphate:polyprenyl phosphate GlcNAc-1-phosphotransferase (AglH) indeed catalyses the first step of the protein *N*-glycosylation process. A gene deletion plasmid was used for homologous recombination as described previously (Wagner et al. 2009). To construct the deletion plasmid, 800–1000 bp of sequence up- and downstream of *saci0093* was PCR amplified. *Apa*I and *Bam*HI restriction sites were introduced at the 5′ ends of the upstream forward primer (1842) and the downstream reverse primer (1845), respectively. The upstream reverse primer (1843) and the downstream forward primer (1844) were each designed to incorporate 15 bp of the reverse complement strand of the other primer, resulting in a 30 bp overlapping stretch. The up- and downstream fragments were fused by overlapping PCR, using the 3′ ends of the up- and downstream fragments as primers. The resulting PCR product was cloned into plasmid pSAV407 using the restriction enzymes *Apa*I and *Bam*HI, yielding the plasmid pSVA1229. The plasmid was transformed into *Escherichia coli* DH5α cells, which were subsequently plated on LB agar containing 50 mg ml^{-1} ampicillin. The plasmid was confirmed by sequencing. To avoid restriction in *S. acidocaldarius*, the plasmid was methylated by transformation in *E. coli* ER1821 cells containing pM.EsaBC4I, which expresses a methylase (obtained from NEB).

Cloning of *aglH*$_{FLAG}$ into a *S. cerevisiae* expression vector

To verify the proposed enzymatic function of AglH we reasoned that *aglH* might be able to complement a conditional lethal yeast *alg*7 mutant, as has previously been demonstrated for the human Alg7 (Eckert et al. 1998) and the AglH of *M. voltae* (Shams-Eldin et al. 2008). We, therefore, cloned *aglH* fused to a FLAG-tag sequence into the pRS426-MET (Mumberg et al. 1995) expression vector. The *aglH* gene was PCR amplified with forward primer (1755) and reverse primer (1756), introducing *Eco*RI and *Xho*I restriction sites, respectively. The 1756 primer incorporated the FLAG-tag sequence upstream of the *Xho*I restriction site. The digested PCR fragment was cloned into the expression vector pRS426-MET (Mumberg et al. 1995) linearised with the restriction enzymes *Eco*RI and *Xho*I, creating plasmid pSAV1212 (Table 3). The plasmid was transformed into *E. coli* DH5α, and was confirmed by sequencing.

Oligonucleotide-directed mutagenesis of *aglH*$_{FLAG}$

Plasmid pSVA1212 was used as a template for the oligonucleotide-directed mutagenesis of *aglH*$_{FLAG}$. In general, a PCR with a specific forward and reverse primers (Table 2) carrying the nucleotide exchange were used to amplify the gene. The resulting PCR products were digested with *Dpn*I to exclude the methylated template plasmid pSVA1229. After purification, each construct was transformed into *E. coli* DH5α, and platted on selective LB plates containing 50 mg ml^{-1} ampicillin. The exchange of the nucleotides was confirmed by sequencing of the entire *aglH*$_{FLAG}$ gene.

Transformation and selection of *S. acidocaldarius* mutants

Competent cells were obtained according to the protocol of Kurosawa and Grogan (Kurosawa and Grogan 2005). Aliquots containing 400–600 ng of methylated plasmids (pSVA1229 or pSVA1246) were mixed with 50 µl of competent MW001 cells and incubated for 5 min on ice. Electroporation was performed using a Gene pulser II (Bio-Rad, USA) with the input parameters 1.25 kV, 25 mF, 1000 W in 1 mm cuvettes. Immediately after the pulse, 50 µl of a 2 × concentrated recovery solution (1% sucrose, 20 mM β-alanine, 20 mM malate buffer pH 4.5, 10 mM MgSO$_4$) was added and the samples were incubated for 30 min at 75 °C under mild shaking conditions (150 rpm). Prior to plating, additionally 100 µl of heated 2x-concentrated recovery solution was added, and 2 × 100 µl was spread on gelrite plates containing Brock medium supplemented with 0.1% NZ-amine and 0.1% dextrin, lacking uracil. After incubation for 5–7 days at 75 °C, large brownish

Table 2 Oligonucleotide primers used in this study

Primer number	Primer sequence (5′–3′)	Restriction site/amino acid exchange
	Δ*aglH*	
1842	CCCACT<u>GGGCCC</u>GAGAGTGTTAGAAAGAGAAGA	*Apa*I
1843	GGTTATCGTAACCGTCAGGGATACGAGCATTATTTTCTCCTTCTT	
1844	ATGCTCGTATCCCTGACGGTTACGATAACCATCTAATGATATACA	
1845	CGCCGA<u>GGATCC</u>TCAACGTGGAATTCCCTCTCC	*Bam*HI
	*aglH*_{FLAG}	
1755	GCGG<u>GAATTC</u>ATGCTCGTATCCCTGCTTGGTATTC	*Eco*RI
1756	GGCG<u>CTCGAG</u>TTACTTGTCATCGTCCTTGTAGTCAATGATGGTTATCGTAACCGT TTG	*Xho*I-FLAG
	*aglH*_{FLAG} point mutation	
2740	GGTTTTACAGGGAAGG<u>C</u>TATAAATAAATTGACTAAG	D039A
2741	CATCATCCTTAGTCAATTTATTTAT<u>AG</u>CCTTCCC	D039A
2742	CTTGGTCTACTTGATG<u>C</u>TATTTTCAACATAAGCCAG	D100A
2743	GTTGAAAAT<u>AG</u>CATCAAGTAGACCAAGAAAACC	D100A
2758	GGGAAGGACATAAAT<u>GC</u>ATTGACTAAGGATGATGTTCC	K042A
2759	CCTTAGTCAAT<u>GC</u>ATTTATGTCCTTCCCTGTAAAACC	K042A
2760	CTTGATGACATTTTC<u>GCC</u>ATAAGCCAGGCTACTAG	N103A
2761	CCTGGCTTATG<u>GC</u>GAAAATGTCATCAAGTAGACC	N103A
2764	CTATCCGGCT<u>GC</u>AACTTTTCCAGGAAATATAGGTAC	K218A
2765	TATTTCCTGGAAAAGTT<u>GC</u>AGCCGGATAGAAATTG	K218A
2766	CAATTTCTATCCGGCTAAAACT<u>GC</u>TCCAGGAAATATAGG	F220A
2767	AATAAAATAAGTACCTATATTTCCTGGA<u>GC</u>AGTTTTAGCCGG	F264A
2768	GATCGTCAATTTTTCCGAACGAGACTCCCTTA<u>GCC</u>CTAGTTTTAG	F264A
	*aglH*_{FLAG}Yeast	
4125	AATCA<u>CTGCAG</u>ATGCTCGTATCCCTGCTTGG	*Pst*I
4126	GGC<u>GGAATTC</u>TTACTTGTCATCGTCGTCCTTGTAGTCAATGATGGTTATCGTAA CCGTTTG	*Eco*RI-FLAG

Mutated nucleotides and restriction sites are *underlined*

colonies were used to inoculate 50 ml of first selection Brock medium containing 0.1% NZ-amine. After 3 days of incubation at 75 °C, each culture was screened for the presence of the integrated plasmid by PCR. Positively tested isolates were inoculated in Brock medium (0.1% NZ-amine and 0.1% dextrin) and grown until an OD_{600} of 0.4 was reached. 40 μl of aliquots were then spread on second selection plates, where the recombination step was selected by the presence of 5-fluoroorotic acid (5-FOA) and uracil. After incubation for 5–7 days at 75 °C, differently sized colonies were picked and streaked onto new second selection plates to ensure single colony formation. Colonies were screened by PCR for the presence or the deletion of *saci0093* (*aglH*), using the outer primers (1842 and 1845).

Transformation and selection of the deletion mutant in YPH 499 *alg*7::HIS3/GAL1-*alg*7

The YPH 499 strain (Mat a; *ura*3–52; *lys*2–801[amber]; *ade*2–101[ochre]; *trp*1-Δ63; *his*3-Δ200; *leu*2-Δ1) (Sikorski and Hieter [1989]) has been used to replace the native *alg*7 promoter with a selection marker/promoter HIS3/GAL1 cassette, resulting in strain YPH 499 *alg*7::HIS3/GAL1-*alg*7 (Mazhari-Tabrizi et al. [1999]). The introduction of the HIS3/GAL1 cassette eliminated the strain's auxotrophy for histidine and placed the *alg*7 gene under the regulation of GAL1. YPH499 was transformed with the plasmid pSVA1212, as described previously (Eckert et al. [1998]) and inoculated on SD medium plates, lacking uracil and histidine.

Immunostaining of the AglH_{FLAG} point mutations expressed in *S. cerevisiae*

Cell pellets of the same OD_{600} from 5 ml of SGR medium cultures of YPH499-HIS-GAL-ALG7 transformed with the AglH complementation plasmids (Table 3) were resuspended in 1 ml of buffer A (100 mM NaCl, 100 mM Tris–HCl, 1 mM EDTA, pH 8) and lysed by 20 min sonification with an intensity of 60% and an interval 20 s (Bandelin Sonopuls). Unbroken cells were removed by centrifugation at 3000×*g* at 4 °C for 20 min. The supernatant was centrifuged in a Beckman Coulter Optima Max-XP Ultracentrifuge at 120,000×*g* at

Table 3 Plasmids used in this study

Plasmid	Genotype	References
pUC18	Cloning vector; Amp^r	Yanisch-Perron et al. (1985)
pSAV407	Gene targeting plasmid, pGEM-T Easy backbone, *pyr*EF cassette of *S. solfataricus*	Wagner et al. (2012)
pSVA1229	Δ*aglH* cloned into pSVA407	This study
pSVA1246	*aglH*$_{STREP}$ cloned into pSVA407	This study
pRS426 MET	Gene targeting and expression vector	Mumberg et al. (1995)
pSVA1212	*aglH*$_{FLAG}$ (Saci0093) cloned into pRS 426 MET with *Xho*I, *Eco*RI	This study
pSVA1247	Based on pSVA1212 containing *aglH*-$_{D039A}$-FLAG	This study
pSVA1248	Based on pSVA1212 containing *aglH*-$_{D100A}$-FLAG	This study
pSVA1258	Based on pSVA1212 containing *aglH*-$_{N103A}$-FLAG	This study
pSVA1259	Based on pSVA1212 containing *aglH*-$_{K218A}$-FLAG	This study
pSVA1260	Based on pSVA1212 containing *aglH*$_{Δ218-329}$	This study
pSVA1261	Based on pSVA1212 containing *aglH*-$_{K042A}$-FLAG	This study
pSVA1262	Based on pSVA1212 containing *aglH*-$_{F264A}$-FLAG	This study
pSVA1263	Based on pSVA1212 containing *aglH*-$_{F220A}$-FLAG	This study
pUC18_*aglH*$_{FLAG}$	Base on pUC18 containing *aglH* from *S. acidocaldarius*	This study

4 °C for 45 min to obtain the membrane pellet. The membrane pellet was resuspended in 0.5 ml of buffer A. Aliquots of 30 μl were loaded on an 11% SDS-PAGE and run at 100 V. The expression of AglH$_{FLAG}$ was analysed by Western immune blotting using the primary antibody anti-DYKDDDDK (Carl Roth, Germany) and an anti-rabbit IgG–alkaline phosphatase-coupled antibody (Sigma Aldrich, St Louis, USA). Chemifluorescence was measured in a Fujifilm LAS-4000 Luminescent image analyzer (Fujifilm, Duesseldorf, Germany).

Results

Identification of AglH, a predicted UDP-GlcNAc-1-phosphate:dolichyl phosphate GlcNAc-1-phosphotransferase

To identify the enzyme required for the first step of the protein *N*-glycosylation pathway in the thermoacidophilic crenarchaeon *S. acidocaldarius,* its genome was analysed for the presence of eukaryotic, bacterial, and archaeal homologues of the UDP-GlcNAc-1-phosphate:dolichyl phosphate GlcNAc-1-phosphotransferase Alg7/Dpagt1, WecA, and AglH, respectively. This search identified *saci0093* (*SACI_RS00435*) encoding a predicted UDP-GlcNAc-1-phosphate:dolichyl phosphate GlcNAc-1-phosphotransferase, which shares 27% amino acid sequence identity with the yeast Alg7 and the human Dpagt1, 31% with AglH from the euryarchaeon *M. voltae* and 26% with WecA of *E.coli*. Saci0093 is located in a gene locus downstream of genes whose products are predicted to be involved in the early steps of isoprenoid lipid biosynthesis (Fig. 1). The gene s*aci0091* (*SACI_RS00425*, *idi*) codes for an isopentenyl diphosphate delta-isomerase, which is necessary for the biosynthesis of isoprenoid compounds via the mevalonate pathway (Boucher et al. 2004). The corresponding protein from *S. shibatae* is an isopentenyl-diphosphate delta-isomerase that catalyses the
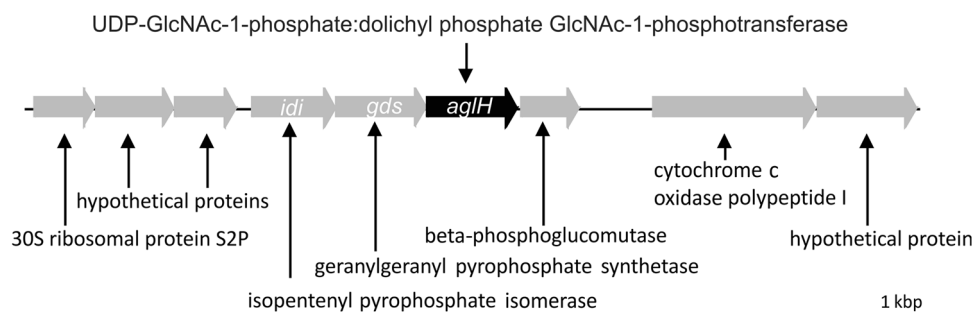

Fig. 1 Physical map of the gene region adjacent to *algH* of *S. acidocaldarius*. Illustrated are the genes *Saci0088* until *Saci0096*. The gene *aglH* displayed in *black* (*saci0093, SACI_RS00435*) encodes the UDP-GlcNAc-1-phosphate:dolichyl phosphate GlcNAc-1-phosphotransferase. The genes *idi* (*saci0091*) and *gds* (*saci0092*) are involved in the isoprenoid lipids biosynthesis

interconversion between two active units for isoprenoid biosynthesis, isopentenyl diphosphate (IPP) and dimethylallyl diphosphate (DMAPP) (Nakatani et al. 2012; Yamashita et al. 2004). Saci0092 (SACI_RS00430, gds) encodes a bifunctional geranylgeranyl pyrophosphate synthase that synthesizes both farnesyl pyrophosphate (FPP) and geranylgeranyl pyrophosphate (GGPP) (Ohnuma et al. 1998; Ohnuma et al. 1996). GGPP is an intermediate for the biosynthesis of many isoprenoid compounds like carotenoids, geranylgeranylated proteins, as well as archaeal ether-linked membrane lipids. Furthermore, GGPP acts as a precursor in the proposed DolP biosynthesis pathway (Guan et al. 2011). Analyses of the Sulfolobales transcriptome revealed a polycistronic mRNA of saci0092 and saci0093 (Wurtzel et al. 2010), indicating a coordinated gene regulation and/or expression for the biosynthesis of DolP and the DolPP-GlcNAc primer in the N-glycosylation process.

AglH from *S. acidocaldarius* shows high similarity in primary sequence and transmembrane topology with eukaryal and bacterial UDP-GlcNAc-1-phosphate:polyprenyl phosphate GlcNAc-1-phosphotransferases

Topology prediction of AglH (Saci0093) in combination with the known primary sequence revealed high levels of similarities with eukaryal as well as bacterial GlcNAc-1-phosphotransferases. AglH possesses ten transmembrane (TM) helices separated by five internal and four external hydrophilic loops (Fig. 2). A similar topology was shown for the eukaryal Alg7 enzyme with ten predicted TM domains, while bacterial WecA typically exhibits ten to eleven TM domains (Anderson et al. 2000; Lehrer et al. 2007). For the archaeal homologue from *M. voltae* only seven TM domains have been predicted (Shams-Eldin et al. 2008). An alignment of AglH with the eukaryal, bacterial,
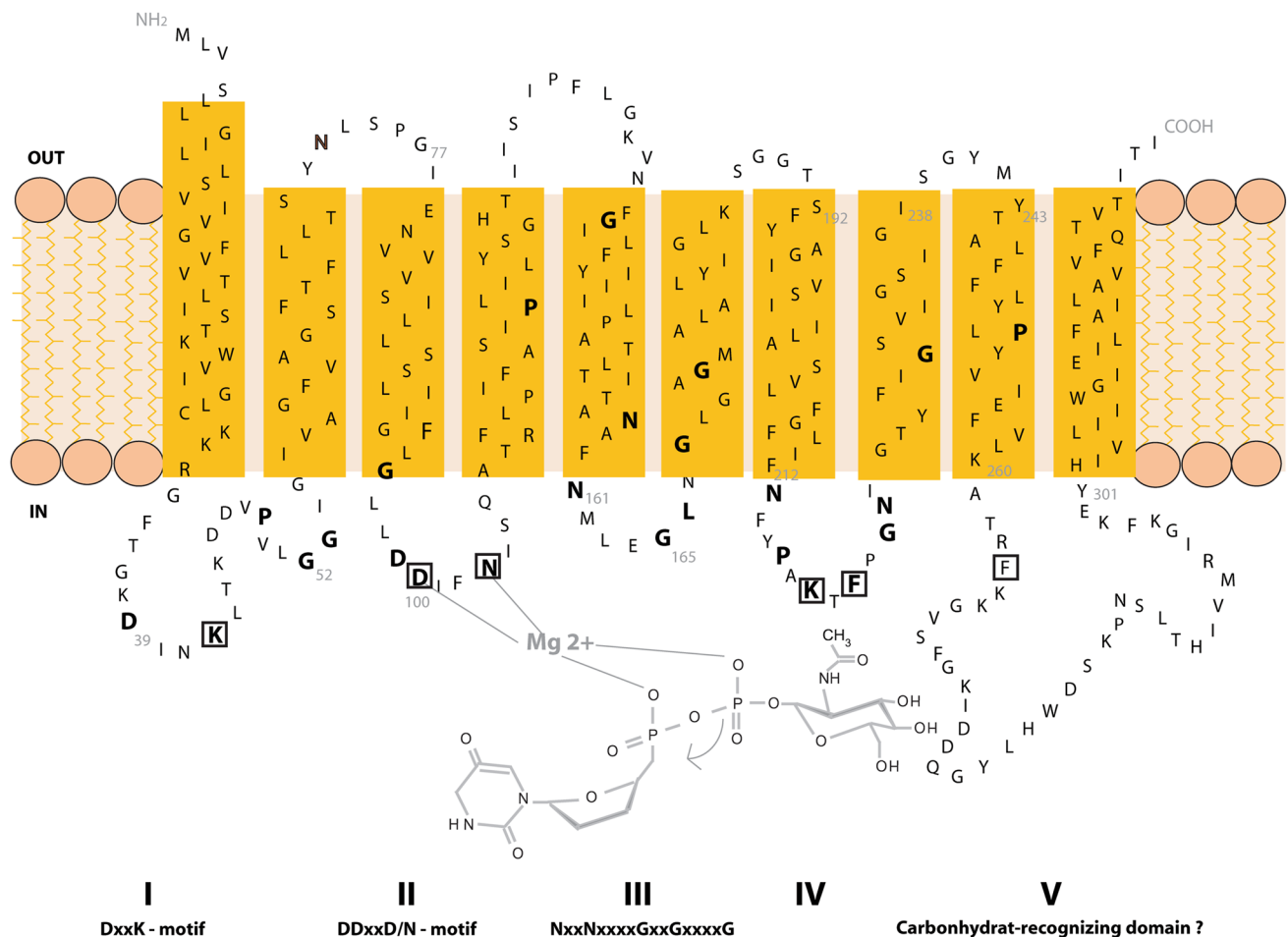

Fig. 2 Topology model of AglH from *S. acidocaldarius*. The topological model was derived using the TMHMM server (http://www.cbs.dtu.dk/services/TMHMM/) and PSIPRED protein structure prediction server (http://bioinf.cs.ucl.ac.uk/psipred/). Conserved amino acids (see alignment Fig. 3) are shown in *bold*. *Numbers* indicate internal cytoplasmic loops I to V, as well as their conserved motifs. Proposed catalytic interaction with UDP-GlcNAc is displayed in *light grey*. *Boxed* amino acids were replaced by alanine

and archaeal orthologues illustrated high amino acid similarity within each of the five cytoplasmic loops, indicating a possibly conserved function across the three domains of life (Fig. 3).

In the cytoplasmic loop (CL) I, a conserved $D_{39}xxK/N$ motif is detected (Figs. 2, 3). In the CL II of Saci0093, a $D_{99}D_{100}xxN_{103}$ motif is present, similar to the conserved motif of eukaryal and bacterial DDxxD motifs (Fig. 3). This conserved motif is potentially involved in Mg^{2+} cofactor binding (Amer and Valvano 2002; Lloyd et al. 2004; Xu et al. 2004). Within the fifth TMD, the CL III, and the six TMD, a long $N_{158}xxN_{161}xxxxG_{165}xxG_{168}xxxxG_{173}$ motif is present. The two conserved aspartic residues have been mutated in the *E. coli* WecA$_{DD156/159GG}$, which resulted in only 3% of the wt transferase activity (Amer and Valvano 2002). The impaired function in vivo and the reduction of enzyme activity in vitro suggest the importance of this motif for the catalytic activity. This motif, in combination with the DDxxK/N motif of the second cytoplasmic loop,

resembles the characteristics of a Walker B motif (Amer and Valvano 2002). The large predicted CL V is thought to be involved in the recognition of the carbohydrate moiety of the UDP-GlcNAc donor. In the respective loop of bacterial WecA, a conserved histidine residue is located within a less conserved short-sequence motif HIHH (Amer and Valvano 2001; Anderson et al. 2000). Replacement of the highly conserved His$_{279}$ residue with serine rendered WecA unable to restore O7 production in an *E. coli* wecA::Tn10 strain (Lehrer et al. 2007). Unlike bacteria, eukaryal and archaeal orthologues are missing the HIHH motif. If the functional interpretation for WecA is correct, this raises the question of how the carbohydrate moiety of the UDP-GlcNAc donor is being recognized in these two domains of life (Fig. 3).

Collectively, the sequence features for AglH are entirely consistent with it being a UDP-GlcNAc-1-phosphate:polyprenyl phosphate GlcNAc-1-phosphotransferase participating in the *N*-glycosylation pathway.
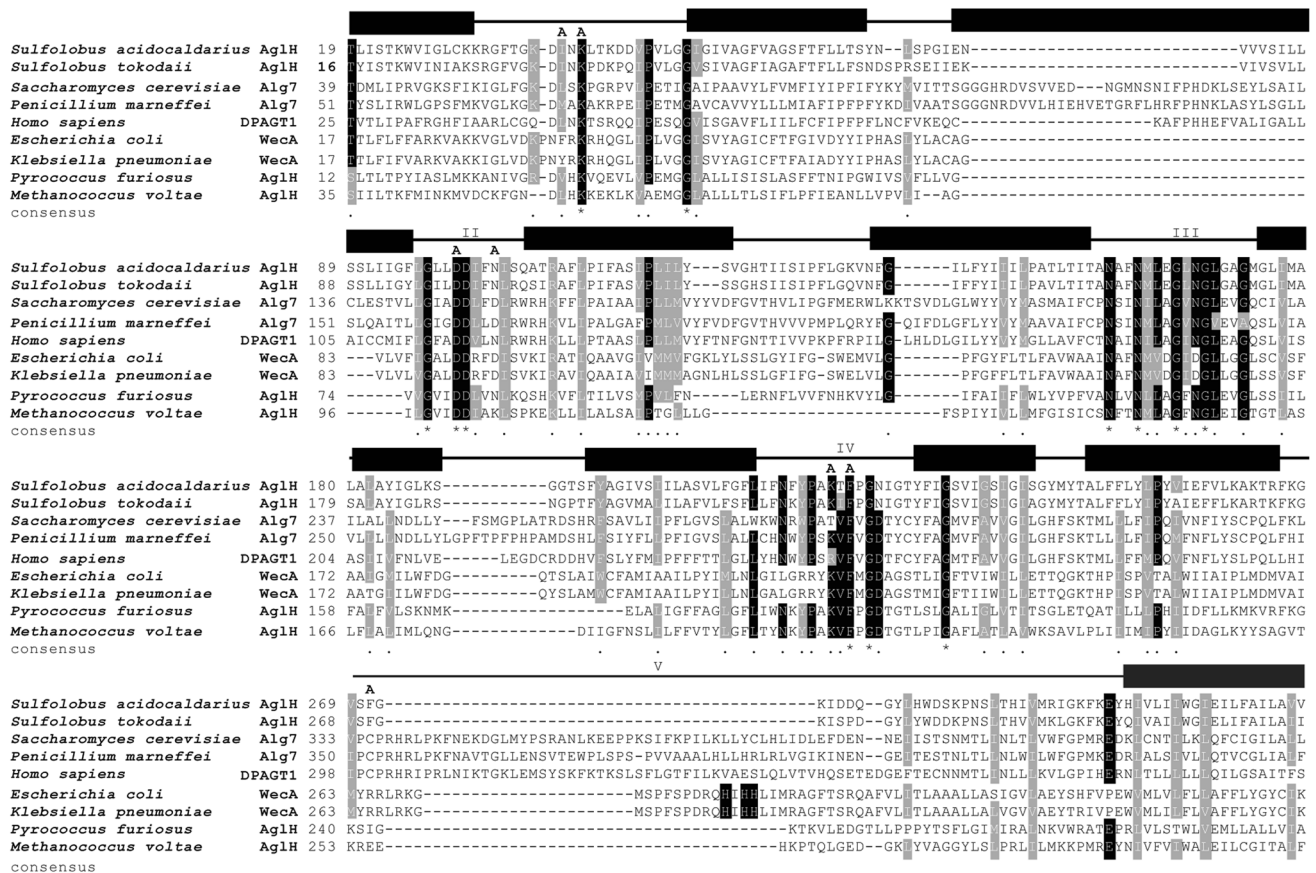

Fig. 3 Alignment of archaeal, bacterial, and eukaryal UDP-GlcNAc-1-P transferase orthologs. Orthologs were identified using BLAST with *S. acidocaldarius* Saci0093 (AglH). Protein sequences were aligned with the ClustalW program. The partial alignment is shown for the region encompassing the conserved motifs DxxK (CL I), DDxxN/D (CL II) and NxxNxxxxGxxGxxxxG (CL III). Conserved amino acids are indicated with asterisks. The boundaries of transmembrane domains (*filled boxes*) and cytosolic loops (*lines*) are shown on *top* of the alignment. The replacement of selected amino acids from AglH of *S. acidocaldarius* by alanine (**a**) are indicated above the sequence

AglH is essential for viability in *S. acidocaldarius*

Based on the obvious conservation of the different motifs within the cytoplasmic loops as well as the characteristic topology profile of AglH (Saci0093), we propose that *algH* indeed encodes a UPD-GlcNAc-1-P transferase initiating the protein *N*-glycosylation process by transferring GlcNAc-1-P from UDP-GlcNAc to DolP. To verify his hypothesis, we designed the plasmid pSVA1229, incorporating the up- and downstream region enclosing Δ*aglH*, to create a markerless deletion mutant of *aglH* in *S. acidocaldarius* by homologues recombination. Integration of this plasmid in *S. acidocaldarius* MW001 was confirmed by PCR using primers encompassing the flanking regions of the target gene. A second homologous recombination, enforced by the addition of 5-fluoroorotic acid, resulted in the segregation of the plasmid, generating either the wild-type stain or the preferred Δ*aglH* deletion strain. Screening of more than 150 different colonies by PCR using primers derived from the flanking regions revealed only the presence of wild-type genetic organization. This result suggests that AglH and *N*-glycosylation process is essential for the archaeon. Polar effects cannot be completely excluded; however, they are unlikely, given the fact that the integration of the plasmid could be achieved and this did not alter the archaeal phenotype. Furthermore, all essential genes for isoprenoid lipid biosynthesis are located upstream of the *aglH*. The segregation of the plasmid would not disturb the genetic neighbourhood, as the integrants did not show any evident alteration in growth.

To underline the essentiality of AglH activity, we explored the growth of *S. acidocaldarius* in the presence of antibiotics interfering specifically with the initiation of the *N*-glycosylation. Tunicamycin, a nucleoside antibiotic, resembles UDP-HexNAc residue and specifically inhibits UDP-HexNAc:polyprenol-P HexNAc-1-P transferases by blocking the active site (Esko and Bertozzi 2009). Bacitracin interferes with the dephosphorylation of isoprenyl pyrophosphate hindering the recycling of new isoprenyl phosphate lipid carrier (Stone and Strominger 1971). The addition of both antibiotics, after reaching early exponential growth phase, showed a dose-dependent reduction of growth of *S. acidocaldarius* (Fig. 4a, b). The addition of 0.3 mM bacitracin ($t_d = 10.7 \pm 0.6$ h) did not significantly reduce the growth compared to the wt doubling time ($t_d = 9.2 \pm 0.9$ h), whereas the addition of 1.2 and 2.4 mM bacitracin decreased the growth two- and fourfold ($t_d = 18.5 \pm 2.5$ h; $t_d = 42.1 \pm 4$ h), respectively. In addition, the addition of tunicamycin reduced the growth rate of *S. acidocaldarius*. Here, 2 μg/ml ($t_d = 13.6$ h ± 1.6) and 6 μg/ml ($t_d = 16.4$ h ± 1.2) led to a significant reduction of growth. Furthermore, the addition of 16 μg/ml increased the doubling time to 40.1 h ± 1.3 for the next 20 h. No growth was detected after 20 h in the samples treated with 16 μg/ml tunicamycin and with the two highest bacitracin concentrations. Interestingly, cells appeared larger compared to wt strain. Thus, the increased OD within the first hours may be attributed to an enlarged cell size. At 32 μg/ml no growth could be detected (Fig. 4b). The effect of the antibiotics inhibiting *N*-glycosylation and thereby inhibiting cell growth was the most obvious when the antibiotics were directly added after inoculation (Fig. 4c). Here, first the OD_{600} slightly increased to 0.1–0.15, then no growth could be detected over 70 h. Based on the reduced stability of the antibiotics (i.e. tunicamycin) at the growth condition (pH 3, 75 °C), the cells recover growth after 70 h.
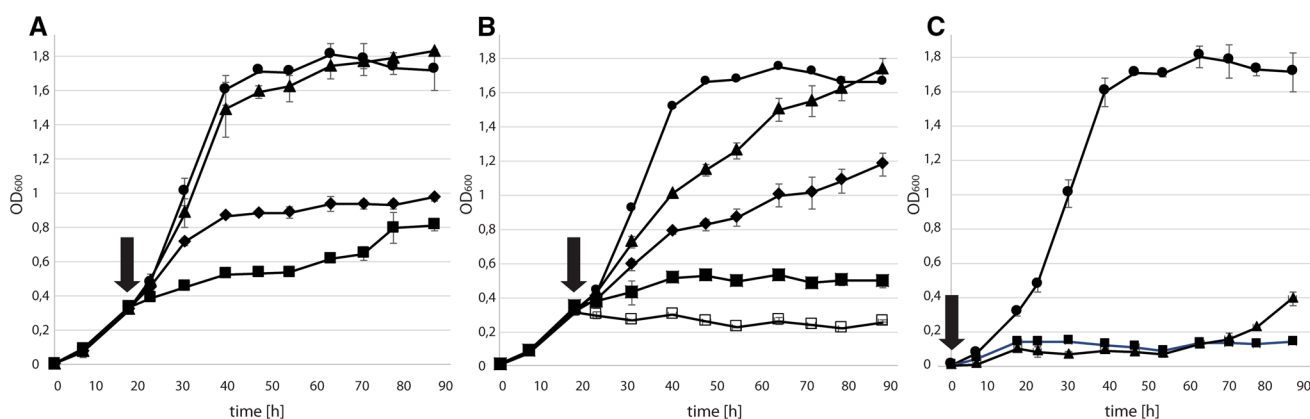

Fig. 4 Effect on the cell growth of *S. acidocaldarius* by the *N*-glycosylation inhibiting antibiotics bacitracin and tunicamycin. **a** Different concentrations of bacitracin: 0 mM (*filled circle*), 0.6 mM (*filled triangle*), 1.2 mM (*filled diamond*), 2.4 mM (*filled square*) mM were added after reaching exponential phase, indicated by *black arrow*. **b** Different concentrations of tunicamycin: 0 (*filled circle*), 2 μg/ml (*filled triangle*), 6 μg/ml (*filled diamond*), 16 μg/ml (*filled square*), 32 μg/ml (*open square*) were added after reaching exponential phase. **c** Cell growth without antibiotics (*filled circle*), with 1.2 mM bacitracin (*filled square*), or 6 μg/ml tunicamycin (*filled triangle*), antibiotics were added directly after inoculation of the culture, indicated by *black arrow*

AglH restores growth of a conditional lethal *alg7* yeast mutant in a complementation assay

To confirm the function of AglH, we tested whether this gene is able to complement a conditional lethal yeast *alg7* mutant, as has been successfully shown for the human *alg7* (Eckert et al. 1998) and *aglH* of *M. voltae* (Shams-Eldin et al. 2008). The full length *algH* gene was cloned into a yeast shuttle vector pRS426Met (Mumberg et al. 1995), containing the selective marker *ura3*$^+$, resulting in the plasmid pSVA1212. After transformation of this plasmid into the conditional lethal yeast *alg7* mutant, YPH499-HIS-GAL-ALG7 (Mazhari-Tabrizi et al. 1999), transformants were plated on SGR as well as SD medium lacking histidine and uracil. Using plates containing either SGR medium (containing galactose) or SD medium (lacking galactose), in which the endogenous yeast *alg7* is expressed or repressed, respectively. Cells transformed with the empty pRS426Met vector served as a negative control and displayed growth only on galactose-containing plates, i.e. conditions under which endogenous *alg7* was expressed (Fig. 5). Under *alg7* repression conditions, this strain failed to grow. Strains containing the plasmid carrying the human *alg7* (positive control) (Eckert et al. 1998) or the *aglH* gene displayed sustained growth on glucose-containing plates, demonstrating the ability of the gene product to functionally replace the essential function of the yeast Alg7 enzyme (Fig. 5). These results showed that *S. acidocaldarius* AglH is indeed functional in *S. cerevisiae* and able to suppress the lethal phenotype of *alg7* by catalysing the transfer of GlcNAc-1-P onto DolP.

Replacement of conserved amino acids resulted in a functional loss of AglH

The complementation assay was employed to verify the functional importance of distinct conserved amino acid residues in the predicted cytoplasmic loops (CL) of *Saci*AglH. The residues mutated were D_{39} and K_{42} in CL I, D_{100} and N_{103} in CL II, K_{218} and F_{220} in CL IV and F_{264} in CL V; all were replaced individually by alanine. Mutations were introduced in the plasmid containing the *aglH* (Saci0093) gene fused to sequences encoding a FLAG epitope tag. The AglH-FLAG fusion protein is fully functional and allows growth of the conditional lethal yeast mutants on SD medium (Fig. 6). Mutations in CL I ($D_{039}A$ and $K_{042}A$) had no effect on the function of the AglHFLAG protein. Also $N_{103}A$ and $K_{218}A$ mutations in CL II and CL III did not affect growth of the yeast mutant. In contrast, the strain complemented with the $D_{100}A$ showed no growth under conditions that repressed the yeast *alg7* gene, implying that D_{100} could be essential for catalysis. The $F_{220}A$ and $F_{264}A$ mutations in CL IV and CL V, respectively, had different effects. While the $F_{220}A$ mutant was substantially impaired in activity as indicated by very poor growth in the complementation assay (Fig. 6), the $F_{264}A$ mutant appeared inactive. To investigate the function of the C-terminal part of the enzyme, a stop codon was introduced at amino acid position 218 AglH$_{\Delta218-329}$. The insertion of a stop codon prevented the ability to functionally complement the Alg7 phenotype. These results showed that the amino acids D_{100}, F_{220} and F_{264} in AglH are important for successful complementation of the lethal phenotype of YPH499-HIS-GAL-ALG7.

Fig. 5 Rescue of a conditional lethal *alg7* yeast mutant by the thermophilic *aglH* from *S. acidocaldarius.* YPH499-HIS-GALprom-ALG7 was transformed with the pRS426-METt plasmids carrying either the human ALG7 (*Hs-alg7*) or the archaeal Saci0093 (*Saci-aglH*). Transformed cells were streaked onto plates containing minimal medium lacking histidine and uracil and containing either galactose or glucose
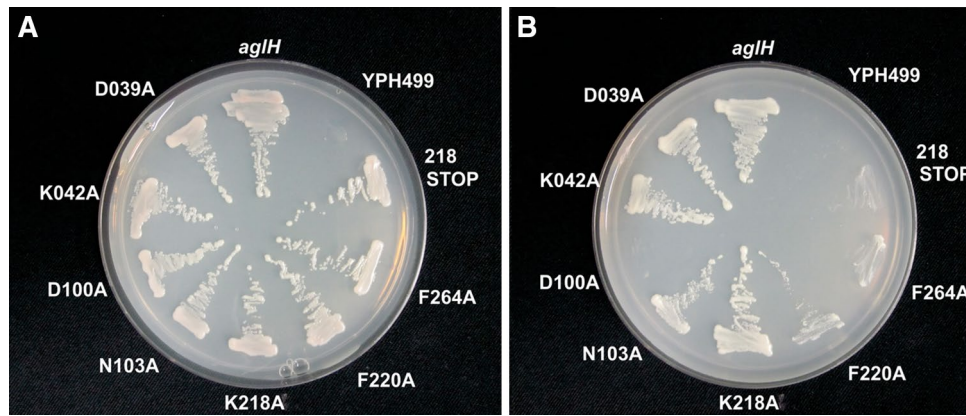
Fig. 6 Functional characterization of AglH in YPH499-HIS-GAL-ALG7 by a complementation assay. The conditional lethal mutant YPH499-HIS-GAL-ALG7 was transformed with the pRS426-METt plasmid carrying either the archaeal *aglH* (Saci0093) or *aglH* with selected point mutations, resulting in the exchange of conserved amino acids to alanine. The transformed cells were then streaked onto plates containing minimal medium lacking histidine as well as uracil and containing either galactose (**a**) or glucose (**b**). The exchange of the conserved amino acids $D_{100}A$, $F_{264}A$ resulted in a lethal, whereas the exchange of $F_{220}A$ resulted in a slow-growing phenotype of YPH499-HIS-GAL, under repression condition of the *alg*7 gene (**b**)

Exchange of conserved amino acid residues did not change the expression level of AglH$_{FLAG}$

To ensure that the AglH$_{FLAG}$ derivatives were expressed and to eliminate the possibility of reduced protein stability due to the amino acid replacements, protein expression was investigated. The membrane fraction of each of the mutated AglH$_{FLAG}$ transformed strains was examined by immuno blotting (Fig. 7). AglH was detected in the wild-type and all mutated AglH$_{FLAG}$ versions, showing that the lack of function observed in Fig. 7 for the $D_{100}A$, $F_{220}A$, and $F_{264}A$ mutations is not caused by reduced protein expression or degraded protein. The observed molecular weight of AglH$_{FLAG}$ corresponds to the calculated molecular weight of 36.6 kDa.

Discussion

Over the last decade, research on archaeal *N*-glycosylation pathways has revealed the diversity of the glycosylation process in terms of the involvement of specific GTases, as well as the structural and compositional complexity of archaeal *N*-glycans (Jarrell et al. 2014). In addition, these studies demonstrated a significant role of glycosylation for the stability of S-layer proteins as well as for the stability and the assembly of the archaellum, the archaeal motility structure (Calo et al. 2010; Yurist-Doutsch et al. 2008). In the thermoacidophilic crenarchaeon family *Sulfolobales*, most if not all surface-exposed proteins (Palmieri et al. 2013), including the S-layer protein (Meyer et al. 2011), the archaellin (Meyer et al. 2013; Meyer et al. 2011), and sugar binding proteins (Elferink et al. 2001), are
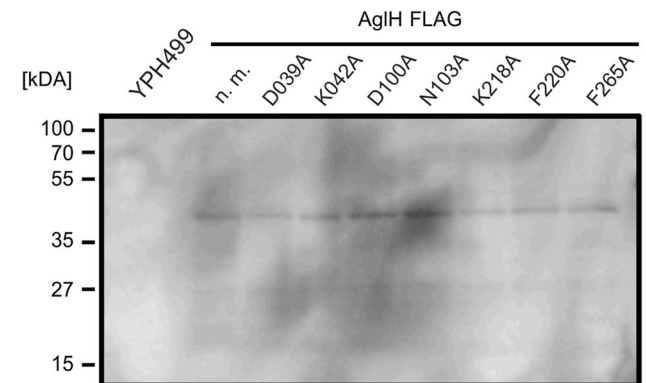

Fig. 7 Detection of the protein expression from the derived AglH$_{FLAG}$ point mutation by Western immunoblotting. Equivalent amounts of cells from YPH499 background strain (*lane 1*) or the complemented strains with the AglH$_{FLAG}$ expression vector (*lane 2–9*) were separated by 11% SDS-PAGE and immunoblotted with antibodies raised against the FLAG-tag epitope. The non-mutated AglH$_{FLAG}$ (n. m.) showed a similar expression level as the different AglH$_{FLAG}$ point mutations (*lane 3–9*)

post-translationally modified by *N*-glycosylation. Defects in *N*-glycan biosynthesis resulted in a significant effect of the growth under elevated salt concentrations as well as a reduced motility (Meyer et al. 2011, 2013).

To understand the *N*-glycosylation in *S. acidocaldarius* in more detail, we searched for the enzyme initiating this process. We identified *aglH* (*saci0093*), coding for a UDP-GlcNAc-1-phosphate:dolichyl phosphate GlcNAc-1-phosphotransferase, which shows high similarities in the overall topology as well as in the amino acid sequence with the eukaryotic Alg7, bacterial WecA, and archaeal homologs (Fig. 3). Based on these structural and sequence

similarities, we analysed whether AglH acts also as a functional homolog by complementation of a conditional *alg7* yeast deletion mutant. Such complementation has been successfully demonstrated previously with the euryarchaeal AglH (Mv1751) from *M. voltae* (Shams-Eldin et al. 2008). Here, we showed that also the thermophilic AglH enzyme complements defects in the biosynthesis of pyrophosphate-linked GlcNAc-isoprenoid units of Eukarya. Although the AglH from *S. acidocladarius* is adapted to high temperatures of around 75 °C, this enzyme is still able to complement the conditional lethal *alg7* yeast mutant restoring the *N*-glycosylation process at 28 °C.

In addition to the ability of AglH to function in Eukarya, we could demonstrate that the substitution of conserved amino acid residues D_{100}, F_{220}, and F_{264} leads to loss of function in the in vivo complementation assay in yeast (Fig. 6). The inability of the AglH $D_{100}A$ mutant to complementing the conditional yeast mutant is consistent with the substitution of the two aspartic acids $DD_{90/91}GG$ in WecA of *E. coli*, where the mutant was impaired in its activity in vitro and in an in vivo complementation system (Amer and Valvano 2002). It is proposed that the DDxxN/D motif and the conserved motif (NxxNxxxGxxGLxxG) of CL III catalyse the formation of the diphosphate linkage of DolPP-GlcNAc (Fig. 3), as the two conserved motifs show sequence similarity to the Walker B motif (Amer and Valvano 2002). The substitution of the highly conserved F_{220} located in the CL IV leads to a drastic reduction in the ability of the AglH to functionally replace Alg7 in yeast. Although little growth could be detected on glucose-containing plates (non-permissive), which is most likely in response to a small amount of Alg7 remaining from the pre-culture on SRG medium, a significantly reduced activity of the AglH $F_{220}A$ is obvious. The data for this mutant align well with the corresponding $F_{249}L$ in eukaryotic UDP-GlcNAc:dolichol-P GlcNAc-1-P transferase (GTP), which resulted in a loss of more than half of the enzymatic activity (Dal Nogare et al. 1998). The function of the less conserved F_{264}, is unclear, but the whole CL V might be involved in the in recognizing the nucleotide-activated sugar donor. Apart from proposed function of the CL V, the overall basic loop might be involved in the oligomerization or interaction with cytosolic GTases. Recently, Alg13/Alg14, which catalyses the second step in eukaryotic *N*-glycan biosynthesis, was found to interact with Alg7. This interaction tethers the soluble Alg13/Alg14 GTases to the membrane of the ER (Lu et al. 2011), which allows the enhanced biosynthesis of the *N*-glycan by clustering the GTase reactions. As *S. acidocaldarius* possesses also a chitobiose core as the *N*-linking unit at the reducing terminus of its *N*-glycan like Eukarya (Peyfoon et al. 2010; Zahringer et al. 2000), a comparable assembly process might also be present in this archaeon. However, bioinformatics searches for an Alg13/Alg14 ortholog in *S. acidocaldarius* failed to identify an *N*-acetylglucosamine transferase.

Deletion of *aglH* was not possible, implicating an essential role of this gene for the viability of *S. acidocaldarius*. This result is consistent with the inability to delete the key enzyme AglB of the *N*-glycosylation process, catalysing the transfer of the oligosaccharide onto target proteins (Meyer and Albers 2014). Treatment with antibiotics directly interfering with the function of AglH function furthermore strengthened the importance of AglH for cell survival (Fig. 4). Studies of the membrane-bound pyrophosphatase SepP (Saci1025) in *S. acidocaldarius,* recycling DolPP back into DolP precursor, revealed the necessity of this DolP cycle (Meyer and Schafer 1992). Here, supplementation of bacitracin interfering with the function of SepP into the growth medium led to the death of the cells, consistent with our findings (Fig. 4). Also treatment with tunicamycin has been previously shown to result in a reduced growth, a gradual increase in cell size, and cell death in *S. acidocaldarius* (Hjort and Bernander 2001). Furthermore, treatment of tunicamycin resulted also in a reduction in the relative amount of glycosylated proteins (Grogan 1996), underlining that this process is indeed important for generating *N*-glycans. However, at that time, no analyses on the lipid-linked glycans confirming the presence of DolPP-linked glycans in *S. acidocaldarius* or other crenarchaeota have been performed. Analyses of the lipid-linked glycans in euryarchaea revealed the presents of DolP rather than DolPP-linked oligosaccharide (Chaban et al. 2009; Guan et al. 2010; Taguchi et al. 2016). In *Hfx. volcanii* and in *M. voltae*, the enzymes AglK and AglJ have been shown to initiate the *N*-glycosylation process by creating DolP-linked glycans, respectively (Kaminski et al. 2010; Chaban et al. 2009; Larkin et al. 2013). Interestingly, besides AglK, a homolog of AglH/Alg7/Dpagt1 has been identified in *M. voltae* (Chaban et al. 2006). A complementation assay in yeast, as it was done in this study, revealed that this AglH is able to replace the function of the eukaryal Alg7, which transfers GlcNAc-1-P from UDP-GlcNAc to DolP, yielding DolPP-GlcNAc (Shams-Eldin et al. 2008). Therefore, it was previously proposed that AglH initiates the *N*-glycosylation in *M. voltae*. However, lipid analyses as well as a detailed biochemical characterisation of AglK and AglH revealed that DolPP-GlcNAc in *M. voltae* is not used for the *N*-glycan assembly, as only DolP-linked oligosaccharides have been detected (Larkin et al. 2013). The study furthermore showed that AglK and AglC, the second enzyme of the *N*-glycosylation pathway, synthesize DolP-GlcNAc-Glc-2,3-diNAcA. This DolP-linked disaccharide is transferred by AglB onto a target peptide in vitro, proving that DolP not only can act as an acceptor but also is used as the glycan donor in *M. voltae* (Larkin et al. 2013).

Here, we proposed that in contrast to euryarchaea the *N*-glycan in crenarchaeon *Sulfolobus* is assembled on DolPP, similar to Eukarya. In fact, two recent studies confirmed the presence of the DolPP-linked *N*-glycans in *Sulfolobales* (Guan et al. 2016; Taguchi et al. 2016). Interestingly the study of Taguchi et al. underlined the difference of the lipid carrier between cren- and euryarchaea, as in all analysed euryarchaea DolP-linked oligosaccharides were present, whereas in the crenarchaea *P. calidifontis* and *S. solfataricus* lipid-linked oligosaccharides were assembled on DolPP backbone (Taguchi et al. 2016). The use of DolPP like in Eukarya emphasises the close evolutionary relationship between Crenachaeota and Eukarya and strengthens the proposed origin of Eukarya from within the TACK super phylum, comprising also the crenarchaeota (Archibald 2008; Guy and Ettema 2011). Interestingly, a newly characterised archaeal phylum, termed Lokiarchaeota, proposed to be one of the deepest branched archaea forms a monophyletic group with eukaryotes in phylogenomic analyses. Within the genomes of these Lokiarchaeota subunits of the eukaryal oligosaccharyltransferase complex are found, i.e. OST3/OST6 (Spang et al. 2015), which had not been found in Archaea so far. This indicates that the archaeon, from which the eukaryotic cell emerged, might have possessed an already highly developed protein *N*-glycosylation pathway.

With this study, we have identified the enzyme that catalyses the first step of the protein *N*-glycosylation process in *S. acidocaldarius*. This will facilitate a more detailed understanding of the archaeal version of this posttranslational modification. Future analyses will be directed to identify additional components of the thermophilic crenarchaeal protein *N*-glycosylation process.

References

Alexander DC, Valvano MA (1994) Role of the *rfe* gene in the biosynthesis of the *Escherichia coli* O7-specific lipopolysaccharide and other O-specific polysaccharides containing *N*-acetylglucosamine. J Bacteriol 176:7079–7084

Amer AO, Valvano MA (2001) Conserved amino acid residues found in a predicted cytosolic domain of the lipopolysaccharide biosynthetic protein WecA are implicated in the recognition of UDP-N-acetylglucosamine. Microbiology 147:3015–3025

Amer AO, Valvano MA (2002) Conserved aspartic acids are essential for the enzymic activity of the WecA protein initiating the biosynthesis of O-specific lipopolysaccharide and enterobacterial common antigen in *Escherichia coli*. Microbiology 148:571–582

Amor PA, Whitfield C (1997) Molecular and functional analysis of genes required for expression of group IB K antigens in *Escherichia coli*: characterization of the his-region containing gene clusters for multiple cell-surface polysaccharides. Mol Microbiol 26:145–161

Anderson MS, Eveland SS, Price NP (2000) Conserved cytoplasmic motifs that distinguish sub-groups of the polyprenol phosphate: *N*-acetylhexosamine-1-phosphate transferase family. FEMS Microbiol Lett 191:169–175

Archibald JM (2008) The eocyte hypothesis and the origin of eukaryotic cells. Proc Natl Acad Sci USA 105:20049–20050

Boucher Y, Kamekura M, Doolittle WF (2004) Origins and evolution of isoprenoid lipid biosynthesis in Archaea. Mol Microbiol 52:515–527

Bouhss A, Trunkfield AE, Bugg TD, Mengin-Lecreulx D (2008) The biosynthesis of peptidoglycan lipid-linked intermediates. FEMS Microbiol Rev 32:208–233

Brock TD, Brock KM, Belly RT, Weiss RL (1972) *Sulfolobus*—new genus of sulfur-oxidizing bacteria living at low pH and high temperature. Arch Microbiol 84:54

Brown S, Zhang YH, Walker S (2008) A revised pathway proposed for *Staphylococcus aureus* wall teichoic acid biosynthesis based on in vitro reconstitution of the intracellular steps. Chem Biol 15:12–21

Bugg TD, Brandish PE (1994) From peptidoglycan to glycoproteins: common features of lipid-linked oligosaccharide biosynthesis. FEMS Microbiol Lett 119:255–262

Burda P, Aebi M (1999) The dolichol pathway of *N*-linked glycosylation. Biochim Biophys Acta 1426:239–257

Calo D, Kaminski L, Eichler J (2010) Protein glycosylation in Archaea: sweet and extreme. Glycobiology 20:1065–1076

Calo D, Guan Z, Naparstek S, Eichler J (2011) Different routes to the same ending: comparing the *N*-glycosylation processes of *Haloferax volcanii* and *Haloarcula marismortui*, two halophilic archaea from the Dead Sea. Mol Microbiol 81:1166–1177

Chaban B, Voisin S, Kelly J, Logan SM, Jarrell KF (2006) Identification of genes involved in the biosynthesis and attachment of *Methanococcus voltae* N-linked glycans: insight into *N*-linked glycosylation pathways in *Archaea*. Mol Microbiol 61:259–268

Chaban B, Logan SM, Kelly JF, Jarrell KF (2009) AglC and AglK are involved in biosynthesis and attachment of diacetylated glucuronic acid to the *N*-glycan in *Methanococcus voltae*. J Bacteriol 191:187–195

Chang MM, Imperiali B, Eichler J, Guan Z (2015) N-linked glycans are assembled on highly reduced dolichol phosphate carriers in the hyperthermophilic archaea *Pyrococcus furiosus*. PLoS One 10:e0130482

Dal Nogare AR, Dan N, Lehrman MA (1998) Conserved sequences in enzymes of the UDP-GlcNAc/MurNAc family are essential in hamster UDP-GlcNAc: dolichol-P GlcNAc-1-P transferase. Glycobiology 8:625–632

Eckert V, Blank M, Mazhari-Tabrizi R, Mumberg D, Funk M, Schwarz RT (1998) Cloning and functional expression of the human GlcNAc-1-P transferase, the enzyme for the committed step of the dolichol cycle, by heterologous complementation in *Saccharomyces cerevisiae*. Glycobiology 8:77–85

Elferink MG, Albers SV, Konings WN, Driessen AJ (2001) Sugar transport in *Sulfolobus solfataricus* is mediated by two families of binding protein-dependent ABC transporters. Mol Microbiol 39:1494–1503

Esko JD, Bertozzi CR (2009) Chemical tools for inhibiting glycosylation. In: Varki A et al (eds) Essentials of glycobiology, 2nd edn. Cold Spring Harbor, New York

Ginsberg C, Zhang YH, Yuan YQ, Walker S (2006) *In vitro* reconstitution of two essential steps in wall teichoic acid biosynthesis. ACS Chem Biol 1:25–28

Glover KJ, Weerapana E, Chen MM, Imperiali B (2006) Direct biochemical evidence for the utilization of UDP-bacillosamine by PglC, an essential glycosyl-1-phosphate transferase in the *Campylobacter jejuni* N-linked glycosylation pathway. Biochemistry 45:5343–5350

Grogan DW (1996) Organization and interactions of cell envelope proteins of the extreme thermoacidophile *Sulfolobus acidocaldarius*. Can J Microbiol 42:1163–1171

Guan ZQ, Naparstek S, Kaminski L, Konrad Z, Eichler J (2010) Distinct glycan-charged phosphodolichol carriers are required for the assembly of the pentasaccharide *N*-linked to the *Haloferax volcanii* S-layer glycoprotein. Mol Microbiol 78:1294–1303

Guan Z, Meyer BH, Albers SV, Eichler J (2011) The thermoacidophilic archaeon *Sulfolobus acidocaldarius* contains an unusually short, highly reduced dolichyl phosphate. Biochim Biophys Acta 1811:607–616

Guan Z, Delago A, Nussbaum P, Meyer B, Albers SV, Eichler J (2016) *N*-glycosylation in the thermoacidophilic archaeon *Sulfolobus acidocaldarius* involves a short dolichol pyrophosphate carrier. FEBS Lett 590:3168–3178

Guy L, Ettema TJ (2011) The archaeal 'TACK' superphylum and the origin of eukaryotes. Trends Microbiol 19:580–587

Hartmann E, König H (1989) Uridine and dolichyl diphosphate activated oligosaccharides are intermediates in the biosynthesis of the S-layer glycoprotein of *Methanothermus fervidus*. Arch Microbiol 151:274–281

Hjort K, Bernander R (2001) Cell cycle regulation in the hyperthermophilic crenarchaeon *Sulfolobus acidocaldarius*. Mol Microbiol 40:225–234

Jaeken J, Matthijs G (2007) Congenital disorders of glycosylation: a rapidly expanding disease family. Annu Rev Genom Hum Genet 8:261–278

Jarrell KF, Ding Y, Meyer BH, Albers SV, Kaminski L, Eichler J (2014) N-Linked glycosylation in Archaea: a structural functional, and genetic analysis. Microbiol Mol Biol Rev MMBR 78:304–341

Kaminski L et al (2010) AglJ adds the first sugar of the *N*-linked pentasaccharide decorating the *Haloferax volcanii* S-layer glycoprotein. J Bacteriol 192:5572–5579

Kurosawa N, Grogan DW (2005) Homologous recombination of exogenous DNA with the *Sulfolobus acidocaldarius* genome: properties and uses. FEMS Microbiol Lett 253:141–149

Larkin A, Imperiali B (2011) The expanding horizons of asparagine-linked glycosylation. Biochemistry 50:4411–4426

Larkin A, Chang MM, Whitworth GE, Imperiali B (2013) Biochemical evidence for an alternate pathway in N-linked glycoprotein biosynthesis. Nat Chem Biol 9:367–373

Lehrer J, Vigeant KA, Tatar LD, Valvano MA (2007) Functional characterization and membrane topology of *Escherichia coli* WecA, a sugar-phosphate transferase initiating the biosynthesis of enterobacterial common antigen and O-antigen lipopolysaccharide. J Bacteriol 189:2618–2628

Lehrman MA (1991) Biosynthesis of *N*-acetylglucosamine-P-P-dolichol, the committed step of asparagine-linked oligosaccharide assembly. Glycobiology 1:553–562

Lloyd AJ, Brandish PE, Gilbey AM, Bugg TD (2004) Phospho-*N*-acetyl-muramyl-pentapeptide translocase from *Escherichia coli:* catalytic role of conserved aspartic acid residues. J Bacteriol 186:1747–1757

Lu J et al (2011) Alg14 organizes the formation of a multi-glycosyltransferase complex involved in initiation of lipid-linked oligosaccharide biosynthesis. Glycobiology 22(4):504–516

Mancuso DJ, Chiu TH (1982) Biosynthesis of glucosyl monophosphoryl undecaprenol and its role in lipoteichoic acid biosynthesis. J Bacteriol 152:616–625

Masson L, Holbein BE (1985) Role of lipid intermediate(S) in the synthesis of serogroup-B *Neisseria meningitidis* capsular polysaccharide. J Bacteriol 161:861–867

Mazhari-Tabrizi R, Blank M, Mumberg D, Funk M, Schwarz RT, Eckert V (1999) Chromosomal promoter replacement in *Saccharomyces cerevisiae*: construction of conditional lethal strains for the cloning of glycosyltransferases from various organisms. Glycoconj J 16:673–679

Mclachlan KR, Krag SS (1992) Substrate specificity of normalacetylglucosamine 1-phosphate transferase activity in chinese hamster ovary cells. Glycobiology 2:313–319

Meier-Dieter U, Barr K, Starman R, Hatch L, Rick PD (1992) Nucleotide sequence of the *Escherichia coli rfe* gene involved in the synthesis of enterobacterial common antigen. Molecular cloning of the rfe-rff gene cluster. J Biol Chem 267:746–753

Meyer BH, Albers SV (2013) Hot and sweet: protein glycosylation in Crenarchaeota. Biochem Soc Trans 41:384–392

Meyer BH, Albers SV (2014) AglB, catalyzing the oligosaccharyl transferase step of the archaeal N-glycosylation process, is essential in the thermoacidophilic crenarchaeon *Sulfolobus acidocaldarius*. Microbiologyopen

Meyer W, Schafer G (1992) Characterization and purification of a membrane-bound archaebacterial pyrophosphatase from *Sulfolobus acidocaldarius*. Eur J Biochem 207:741–746

Meyer BH et al (2011) Sulfoquinovose synthase—an important enzyme in the *N*-glycosylation pathway of *Sulfolobus acidocaldarius*. Mol Microbiol 82:1150–1163

Meyer BH et al (2013) Agl16, a thermophilic glycosyltransferase mediating the last step of N-glycan biosynthesis in the thermoacidophilic crenarchaeon *Sulfolobus acidocaldarius*. J Bacteriol 195:2177–2186

Mumberg D, Muller R, Funk M (1995) Yeast vectors for the controlled expression of heterologous proteins in different genetic backgrounds. Gene 156:119–122

Nakatani H, Goda S, Unno H, Nagai T, Yoshimura T, Hemmi H (2012) Substrate-induced change in the quaternary structure of type 2 isopentenyl diphosphate isomerase from *Sulfolobus shibatae*. J Bacteriol

Ohnuma S, Hirooka K, Hemmi H, Ishida C, Ohto C, Nishino T (1996) Conversion of product specificity of archaebacterial geranylgeranyl-diphosphate synthase. Identification of essential amino acid residues for chain length determination of prenyltransferase reaction. J Biol Chem 271:18831–18837

Ohnuma S, Hemmi H, Koyama T, Ogura K, Nishino T (1998) Recognition of allylic substrates in *Sulfolobus acidocaldarius* geranylgeranyl diphosphate synthase: analysis using mutated enzymes and artificial allylic substrates. J Biochem 123:1036–1040

Palmieri G, Balestrieri M, Peter-Katalinic J, Pohlentz G, Rossi M, Fiume I, Pocsfalvi G (2013) Surface-exposed glycoproteins of hyperthermophilic *Sulfolobus solfataricus* P2 show a common glycosylation profile. J Proteome Res

Paul G, Wieland F (1987) Sequence of the halobacterial glycosaminoglycan. J Biol Chem 262:9587–9593

Peyfoon E et al. (2010) The S-layer glycoprotein of the crenarchaeote *Sulfolobus acidocaldarius* is glycosylated at multiple sites with chitobiose-linked *N*-glycans. Archaea

Samuel G, Reeves P (2003) Biosynthesis of O-antigens: genes and pathways involved in nucleotide sugar precursor synthesis and O-antigen assembly. Carbohydr Res 338:2503–2519

Schmidt G, Mayer H, Makela PH (1976) Presence of *rfe* genes in *Escherichia coli*—their participation in biosynthesis of O antigen and enterobacterial common antigen. J Bacteriol 127:755–762

Shams-Eldin H, Chaban B, Niehus S, Schwarz RT, Jarrell KF (2008) Identification of the archaeal *alg*7 gene homolog (encoding *N*-acetylglucosamine-1-phosphate transferase) of the *N*-linked glycosylation system by cross-domain complementation in *Saccharomyces cerevisiae*. J Bacteriol 190:2217–2220

Sikorski RS, Hieter P (1989) A system of shuttle vectors and yeast host strains designed for efficient manipulation of DNA in *Saccharomyces cerevisiae*. Genetics 122:19–27

Spang A et al (2015) Complex archaea that bridge the gap between prokaryotes and eukaryotes. Nature 521:173–179

Stone KJ, Strominger JL (1971) Mechanism of action of bacitracin: complexation with metal ion and C 55-isoprenyl pyrophosphate. Proc Natl Acad Sci USA 68:3223–3227

Taguchi Y, Fujinami D, Kohda D (2016) Comparative analysis of archaeal lipid-linked oligosaccharides that serve as oligosaccharide donors for Asn glycosylation. J Biol Chem 291:11042–11054

Troy FA, Vijay IK, Tesche N (1975) Role of undecaprenyl phosphate in synthesis of polymers containing sialic acid in *Escherichia coli*. J Biol Chem 250:156–163

Typas A, Banzhaf M, Gross CA, Vollmer W (2012) From the regulation of peptidoglycan synthesis to bacterial growth and morphology. Nat Rev Microbiol 10:123–136

Wagner M, Berkner S, Ajon M, Driessen AJ, Lipps G, Albers SV (2009) Expanding and understanding the genetic toolbox of the hyperthermophilic genus *Sulfolobus*. Biochem Soc Trans 37:97–101

Wagner M, van Wolferen M, Wagner A, Lassak K, Meyer BH, Reimann J, Albers SV (2012) Versatile genetic tool Box for the crenarchaeote *Sulfolobus acidocaldarius*. Front Microbiol 3:214

Whitfield C (2006) Biosynthesis and assembly of capsular polysaccharides in *Escherichia coli*. Annu Rev Biochem 75:39–68

Wurde AE et al. (2012) Congenital disorder of glycosylation type Ij (CDG-Ij, DPAGT1-CDG): extending the clinical and molecular spectrum of a rare disease. Mol Genet Metab

Wurtzel O, Sapra R, Chen F, Zhu Y, Simmons BA, Sorek R (2010) A single-base resolution map of an archaeal transcriptome. Genome Res 20:133–141

Xu L, Appell M, Kennedy S, Momany FA, Price NPJ (2004) Conformational analysis of chirally deuterated tunicamycin as an active site probe of UDP-*N*-Acetylhexosamine: polyprenol-P *N*-acetylhexosamine-1-P translocases. Biochemistry 43:13248–13255

Yamashita S, Hemmi H, Ikeda Y, Nakayama T, Nishino T (2004) Type 2 isopentenyl diphosphate isomerase from a thermoacidophilic archaeon *Sulfolobus shibatae*. Eur J Biochem 271:1087–1093

Yanisch-Perron C, Vieira J, Messing J (1985) Improved M13 phage cloning vectors and host strains: nucleotide sequences of the M13mp18 and pUC19 vectors. Gene 33:103–119

Yurist-Doutsch S, Chaban B, VanDyke DJ, Jarrell KF, Eichler J (2008) Sweet to the extreme: protein glycosylation in Archaea. Mol Microbiol 68:1079–1084

Zahringer U, Moll H, Hettmann T, Knirel VA, Schafer G (2000) Cytochrome $b_{558/566}$ from the archaeon *Sulfolobus acidocaldarius* has a unique Asn-linked highly branched hexasaccharide chain containing 6-sulfoquinovose. Eur J Biochem 267:4144–4149